


M.B. PUSHKARSKY
M.E. WEBBER 
O. BAGHDASSARIAN
L.R. NARASIMHAN
C.K.N. PATEL

Laser-based photoacoustic ammonia sensors for industrial applications

Pranalytica Inc., 1101 Colorado Ave., Santa Monica, CA 90401, USA

Received: 3 April 2002/Revised version: 31 May 2002
Published online: 21 August 2002 • © Springer-Verlag 2002

ABSTRACT An industrial trace-ammonia sensor based on photoacoustic spectroscopy and CO₂ lasers has been developed for measuring ammonia with a 1σ detection limit of 220 parts-per-trillion (ppt) in an integration time of 30 s. The instrument response time for measuring ammonia was 200 s, limited by adsorption effects due to the polar nature of ammonia. The minimum detectable fractional absorbance was 2.0×10^{-7} , and the minimum normalized detectable absorption coefficient for this system was $2.4 \times 10^{-7} \text{ W cm}^{-1}/\sqrt{\text{Hz}}$. The $9R(30)$ transition of the CO₂ laser at $9.22 \mu\text{m}$ with 2 W of output power was used to probe the strong $sR(5,K)$ multiplet of ammonia at the same wavelength. This sensor was demonstrated with an optically multiplexed configuration for simultaneous measurement in four cells.

PACS 42.62.F; 82.80.G; 82.80.K

1 Introduction

Ammonia is in widespread use worldwide for a variety of industrial applications, including refrigeration, refining, manufacturing and cleaning. Moreover, ammonia is the primary basic gas and third-most abundant nitrogen-containing compound in the atmosphere [1]. As a result of ammonia's widespread use, toxicity and contaminating effect on deep-UV wafer lithography, ammonia sensing is relevant to a variety of industrial applications, including leak detection at chiller plants, ambient build-up monitoring at agricultural facilities such as feed lots, and for contaminant monitoring in semiconductor clean rooms.

For the semiconductor clean room applications, the presence of ammonia gases at concentrations greater than 10 parts-per-billion (ppb) can detrimentally affect wafer yields at facilities that use deep-UV lithography due to damage that occurs to the optical components and the chemically amplified resists [2, 3]. Thus, sensors are needed that can selectively measure ammonia at sub-ppb levels continuously and autonomously without frequent calibration, in order to avoid expensive damage to fabrication lines and to prevent

unnecessary shutdowns due to high levels of contamination. These criteria make laser-based techniques an attractive alternative to the existing "gold standard" sensing benchmark, chemiluminescence, which has a detection limit of roughly 0.5 ppb, but is subject to false signals from nitrogen-containing compounds such as NO and amines. This paper discusses the development of a multiplexed CO₂-laser-based photoacoustic sensor for semiconductor clean room applications that can detect ammonia at sub-parts-per-billion (ppb) levels simultaneously in four sample streams with an integration time of 30 s and an instrument response time of a few minutes. This work also demonstrates the resonant operation of the sensor over several hours to determine the minimum detectivity based on replicate precision of successive measurements.

2 Photoacoustic spectroscopy

Of the many different laser-based sensing techniques available for development into an instrument that can autonomously detect sub-ppb concentrations, photoacoustic spectroscopy is especially well suited due to its relative simplicity, ruggedness and overall sensitivity. Photoacoustic spectroscopy is a well-established technique with many publications available that describe its theory and various implementations in great detail [4–7]. In brief, photoacoustic spectroscopy is an absorption-based diagnostic tool that involves four steps (see Fig. 1):

1) Modulation of the laser radiation (either in frequency or amplitude) at a wavelength that overlaps with a spectral feature of the target species.

2) Excitation of the target molecule by absorption of the incident radiation.

3) Deactivation of the excited molecule via collisions, during which the absorbed radiation energy is converted into periodic local heating at the modulation frequency.

4) Monitoring the resulting acoustic waves with a microphone.

The following wave equation governs the conversion of heat input from incident laser radiation into acoustic waves [6]:

$$\nabla^2 P - \frac{1}{c^2} \frac{\delta^2 P}{\delta t^2} = -\frac{(\gamma - 1)}{c^2} \frac{\delta H}{\delta t} \quad (1)$$

✉ Fax: +1-310/458-0171, E-mail: webber@pranalytica.com

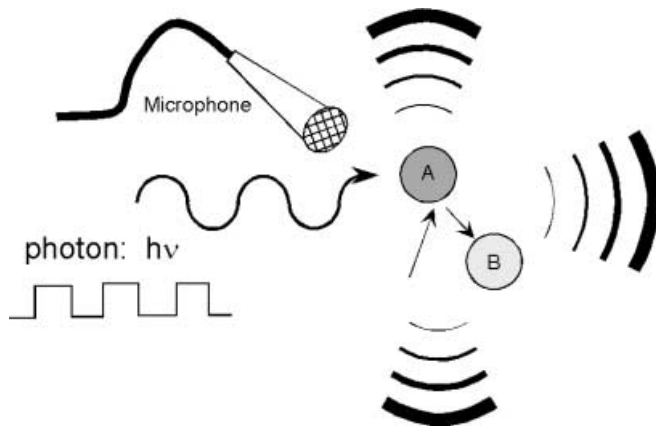


FIGURE 1 Photoacoustic signal is generated by modulated radiation that is absorbed by molecule A, then converted from collisions with molecule B into local heating and acoustic waves that can be detected with a microphone

The term on the right-hand side of the equation describes the changes in heat input with time. When the heat input is constant, this term is zero and no pressure wave is generated. Thus, the heat input must be modulated, which requires that the laser radiation must also be modulated, either in amplitude or frequency. The magnitude of the photoacoustic signal that results from absorption followed by deactivation is described by:

$$S = CPN\sigma\Delta tS_m \quad (2)$$

where C is a cell-specific constant, P is the power of the incident laser radiation, N is the number density of absorbing molecules, σ is the absorption cross section of the transition that is being interrogated, Δt is the cycle period of the modulated radiation, and S_m is the sensitivity of the microphone [8].

Equation (2) reveals that the photoacoustic signal is linearly dependent on laser power. Thus, sensitive measurements benefit from using as much laser power as is reasonably available. Moreover, the signal is directly dependent on the number of molecules in the optical path, which means that this technique is truly a “zero-baseline” strategy, since to first order, no signal will be generated if the target molecules are not present. The Δt term indicates that for non-resonant operation, the signal goes down at higher modulation frequencies. As a result, most non-resonant measurements are made with modulation frequencies between 10 and 100 Hz [9]. Unfortunately, $1/f$ noise is also higher in this measurement regime. The cell-specific constant, C , is more complicated, and is not really a constant at all, but rather is a function of cell geometry, measurement conditions and the modulation frequency. For some measurement cells that are used as acoustic resonators, longitudinal, radial or azimuthal modes naturally enhance the cell-parameter C at specific frequencies such that signals become significantly larger than for non-resonant operation, despite the inverse dependence from the Δt term on the signal. This phenomenon is illustrated nicely by Fig. 5.2 in [4] and Fig. 1 in [7], both of which show strong resonant responses between 1 and 8 kHz.

The amount of signal enhancement that occurs when the laser is modulated at a resonant frequency is determined by the quality factor, Q , which is the resonant frequency, f_0 , nor-

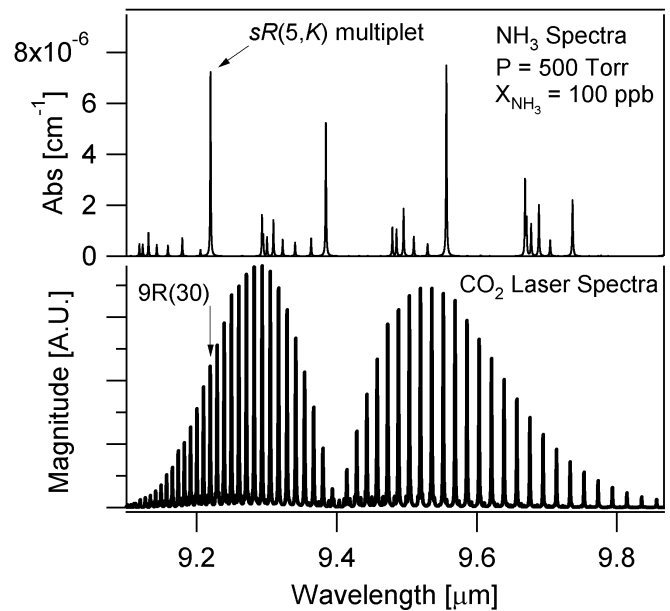


FIGURE 2 The CO₂ laser 9R(30) transition near 9.22 μm overlaps with the very strong $sR(5, K)$ multiplet spectral feature of ammonia [12]

malized by the half width of the resonance profile, Δf :

$$Q = \frac{f_0}{\Delta f} \quad (3)$$

The half width refers to the width of the resonance profile at half the intensity, and is measured between the points where the photoacoustic amplitude of the resonance profile is at $1/\sqrt{2}$ the peak value. Q is typically between 10 and 50 for longitudinal resonators, but can be as high as 1000 for spherical cavities [9].

Including the contributions of resonance, the photoacoustic signal described in (2) can be simplified at one operating frequency to:

$$S = S_m PC\alpha \quad (4)$$

where the microphone sensitivity at the activation frequency, S_m , is in units of volts per pascal; the power, P is in watts; the absorption coefficient α is in inverse centimeters; and the cell constant, C , has units of pascal centimeters per watt. Equation (4) thus yields the photoacoustic signal in volts, which is linearly dependent on the microphone sensitivity, incident laser power, absorption coefficient and cell factor. Thus, by doubling Q , the microphone sensitivity, the laser power or the number of absorbing molecules in the optical path, the voltage will also double.

In addition to its sensitivity and zero-baseline attributes, another advantage of photoacoustic spectroscopy for trace gas analysis is that as the laser beam passes through the sample cell, very few photons are absorbed, and thus the transmitted beam typically has sufficient power, even after the losses from absorption in the windows and their coatings, for interrogating samples in successive cells via an optical multiplexing arrangement. A multiplexed photoacoustic sensor can be used to monitor many different samples simultaneously so that one instrument can be deployed to monitor up to 20 different

points within a clean room, industrial plant or other facility. Moreover, since so few photons are absorbed, the detection is typically linear over five orders of magnitude, and thus shows magnificent dynamic range, until it becomes non-linear for optical densities greater than about 6% [10].

As with many other optical techniques, the ultimate sensitivity is a valuable parameter, and such a value is typically estimated by measuring the signal-to-noise ratio (SNR). For photoacoustic spectroscopy, however, the “noise” often has a structure that is coherent with the signal from the target species, and therefore it should be treated more accurately as a background signal, not as a noise. The background signal can be established by measuring the acoustic signal in the absence of absorbers (i.e. with pure nitrogen), but with the same flow and pressure conditions as those for the sample gases.

3 Laser sources

One laser that has a long history in the field of trace-gas detection using photoacoustic spectroscopy is the CO₂ laser, whose high powers and access to strong absorption transitions for species such as ammonia, benzene and ethylene has yielded many sensitive gas detectors since the early-1970s [11]. The use of CO₂ lasers for photoacoustic trace-gas detection has been well established [5], but has not been typically incorporated into commercially available gas-sensing instruments because of the power requirements and size of traditional tabletop CO₂ lasers. However, the recent commercial availability of sealed-off, low-power (< 25 W), grating-tunable CO₂ lasers enables the development of instrumentation with excellent sensitivity and compact footprints that can be readily deployed in industrial or medical settings.

CO₂ lasers operate at approximately 120 discrete wavelengths between 9 and 11 μm. These transitions are separated by 1–2 cm⁻¹ and the laser frequency, therefore, is not continuously tunable. However, by employing appropriate pressure broadening of the absorbing species, spectral overlap with CO₂ laser frequencies can be achieved. A CO₂ laser is especially useful for detecting NH₃ because one of its laser lines, the 9R(30) transition near 9.22 μm, is nearly coincident with one of ammonia’s strongest spectral features (see Fig. 2). This particular feature is the sR(5, K) multiplet and is a combination of six different transitions. Though the ammonia feature near 9.55 μm is also very strong, its overlap with a CO₂ laser wavelength is inferior to the multiplet at 9.22 μm. The absorption coefficient at the center of the CO₂ laser’s gain profile for the feature at 9.22 μm, as calculated by summing the contributions from six individual Voigt profiles for a pressure of 500 Torr, is approximately 99 cm⁻¹atm⁻¹ [9, 12]. Despite the high output power and transition strength, this system will not be affected by saturation of the upper state at this pressure unless the output power is increased by a few orders of magnitude.

CO₂ lasers are one of the oldest types of laser (invented in 1964), and enjoy wide implementation worldwide for a variety of applications. More than 10 450 CO₂ lasers were shipped in 2001, which makes them the world’s second most popular laser after semiconductor diodes. Thus, lasers from many different vendors and with widely varying powers and sizes are available for incorporating in laser-based instrumen-

tation. Moreover, CO₂ lasers have been rated for different strict operating environments, including medical settings, military arenas and space, and thus are suitable for most industrial applications, including clean room deployment. This laser can operate unattended for 15 000 hours, and thus is suitable for the long-lifetime requirements of many sensing systems.

4 Gas handling

Ammonia is a difficult gas to handle reproducibly due to its polar nature, which makes it a very “sticky” molecule that adsorbs to most surfaces. Because of this nature, measurements of ammonia within a mixture of other gases require flowing samples so that the surfaces exposed to ammonia can be passivated as the samples flow by. The net effect is that measurements of ammonia display significant rise times and the materials for handling ammonia mixtures must be selected wisely. Several papers have addressed the complicated issue of ammonia adsorption [9, 13–15]. The rate of ammonia adsorption to the gas handling surfaces is determined by the material of the gas handling surfaces, the mixture concentration, flow rate, pressure and temperature of the surfaces. Moreover, faster flow rates expose more ammonia molecules to the gas handling components, and thus passivate the surfaces more quickly. The rise times are also inversely related to the concentration of ammonia in the mixture: for higher mixture concentrations, more ammonia is available for surface passivation and it occurs more quickly, while for lower concentrations, fewer ammonia molecules are available for passivation. For concentration levels below 100 ppb, these rise times can be several hours for unoptimized systems, but for optimized systems, can be as low as a few minutes.

These same characteristics make it difficult to purchase certified mixtures with ammonia concentrations below 10 ppm. However, for semiconductor clean room application, much lower concentrations (between 1 and 100 ppb) are of interest, and thus we generated our own mixtures with low concentrations for testing purposes using high-precision NIST-traceable mass flow controllers within a gas dilution system. By starting with certified bottles of 10 ppm ammonia mixtures with a balance of nitrogen, gases could be diluted 1000 times with nitrogen such that ammonia concentrations as low as 10 ppb could be generated with an accuracy of approximately ±1 ppb.

5 Instrumentation details

The instrument layout is shown schematically in Fig. 3, and consists of a CO₂ laser, optics for shaping and directing the radiation, four flow-through measurement cells, a laser power meter, lock-in amplifiers for signal conditioning and a computer for controlling the system and analyzing the signals to produce concentration readings in real time. The radiation source is a sealed-off radiofrequency-excited CO₂ laser whose operating wavelength can be line-switched by using an intracavity grating. More than 97% of the laser radiation was transmitted through each cell, which allows for up to 20 cells to be used in series with sufficient power for sensitive measurements.

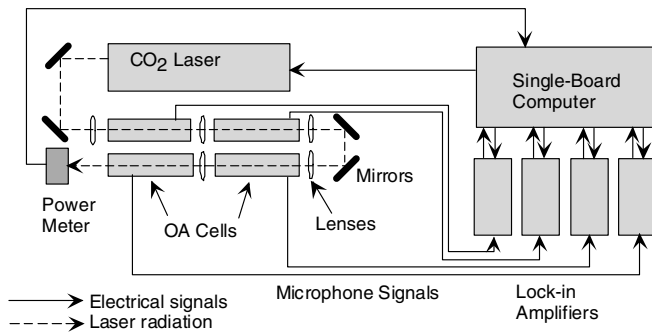


FIGURE 3 Experimental schematic of the multiplexed four-cell configuration, using a single radiation source, four optoacoustic cells, four lock-in amplifiers, one power meter, and one single-board computer

The optoacoustic cell's resonance profile was characterized to determine the frequency of its first longitudinal mode (see Fig. 4) and the value of the cell's quality factor, Q (see Fig. 5). The first longitudinal mode occurs near 1915 Hz and yields optoacoustic signals that are significantly enhanced vis-à-vis non-resonant signals near 100 Hz. The quality factor was measured by tuning the modulation frequency in 10 Hz increments across the resonance profile to estimate the half width, as described above. For this optoacoustic cell, the profile width at half intensity was 38.5 Hz, yielding a quality factor $Q = 49.7$, which is higher than quality factors reported previously by Schmohl, Harren and Bijnen, who obtained values of 17, 32 and 40, respectively [9, 10].

A comparison of microphone signals for non-resonant operation at 100 Hz and resonant operation at 1915 Hz is depicted in the top and bottom panels of Fig. 6. In both cases, the laser was amplitude-modulated with duty cycles between 15 and 25%. For non-resonant operation, the photoacoustic signals exhibit ringing at the resonant frequency on top of the 100-Hz square wave. For resonant operation, the microphone output is simply a coherent sine wave. The data shown in the bottom panel of Fig. 6 were collected with a concentration of approximately 80 ppb ammonia in the optoacoustic cell, which demonstrates the size of the signals after they have been amplified electronically by a factor of 100. As can be

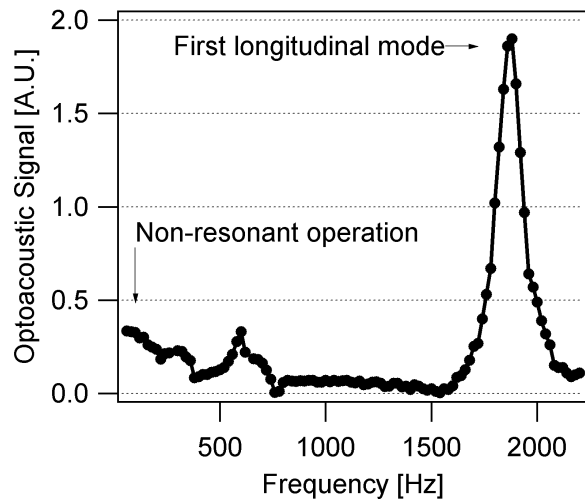


FIGURE 4 The resonance profile for the optoacoustic cell, showing that the resonator's first longitudinal mode occurs near 1900 Hz

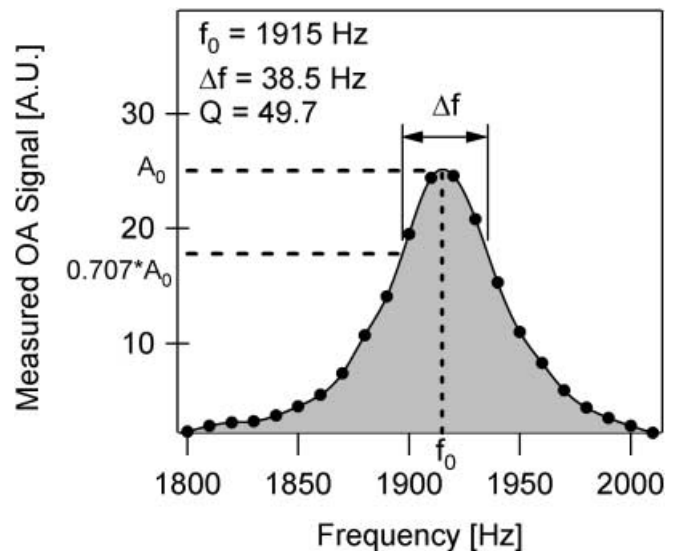


FIGURE 5 Measurements of the resonance profile near the first longitudinal mode to determine the cell's quality factor, Q

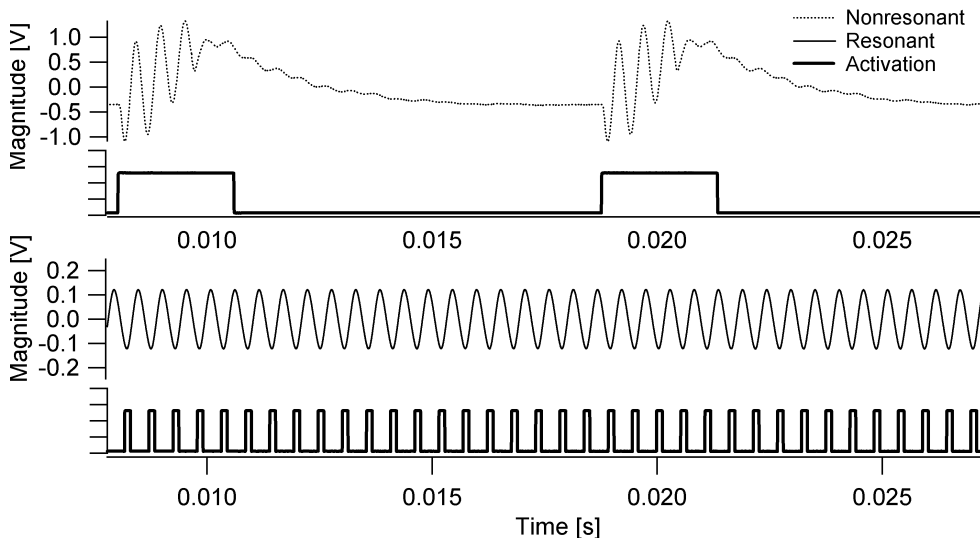


FIGURE 6 Raw microphone signals for non-resonant (top panel) and resonant (bottom panel) operation

seen from the microphone's output, the signals are very clean, and in fact no noise is visible on the sine wave. Unamplified microphone signals have magnitudes of approximately $10\ \mu\text{V}$ for 1 ppb of ammonia with 2 W of laser power. The microphones for the optoacoustic cell have a sensitivity of $22\ \text{mV}/\text{Pa}$ at 1915 Hz, thus the cell factor from (4) at 1915 Hz is $C = 3250\ \text{Pa cm}/\text{W}$.

Flow rates between 200 and 300 sccm were used to minimize rise times due to adsorption effects, and also to prevent excessive flow noise due to turbulence in the cell. Cell pressures ranged from 500 to 760 Torr to ensure sufficient pressure broadening for spectral overlap between the $9R(30)$ laser line and the ammonia spectral feature at $9.22\ \mu\text{m}$. The overall portable sensor system consumed about 150 W of power.

6 Performance and results

This sensor has been demonstrated for sub-ppb sensitivity, as determined by the long-term stability of the instrument when tested with a continuous flow of a calibrated ammonia mixture, with a measurement time of 30 s. Figure 7 shows the results for this instrument measuring ammonia concentration in four cells simultaneously. The cells were tested with flowing ammonia mixtures whose concentration increased in "staircase" fashion with 100-ppb increments, starting at 100 ppb, up to 600 ppb, and then back down to zero.

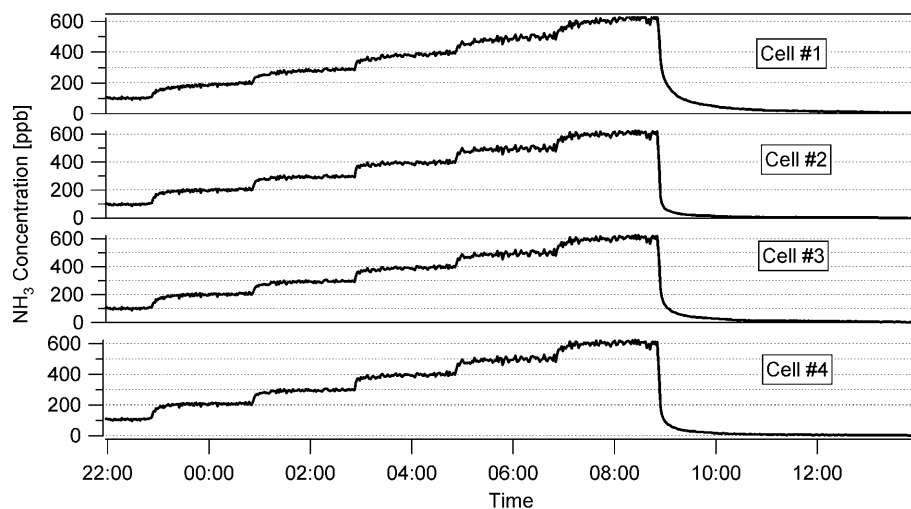


FIGURE 7 Simultaneous measurement in 4 cells through step-wise increments in ammonia concentration from 100 to 600 ppb

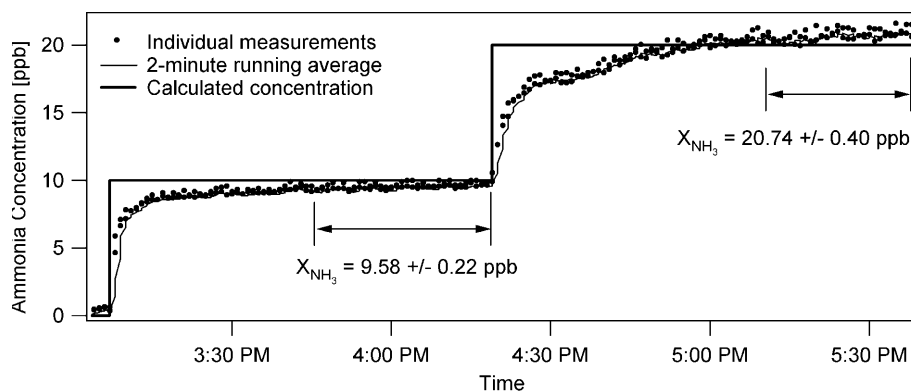


FIGURE 8 Measurements of ammonia concentration in 10 ppb steps from 0 to 20 ppb. Instrument precision is 220 ppt for 10-ppb mixtures, with an accuracy of 4%, possibly limited by the precision of the dilution system

As these results illustrate, all four cells track each other nicely, and the signals respond to varying concentrations with excellent linearity.

Figure 8 shows results from one cell, for clarity, that has been stepped through a staircase with 10-ppb increments from 0 to 20 ppb. These increments were made by flowing pure nitrogen through the cell to purge the system, then switching to a flow with 10-ppb ammonia in a balance of nitrogen. The ammonia mixture had been flowing for more than an hour and was equilibrated before it was switched to flow through the measurement cell. As such, the rise time from 0 to 10 ppb reflects the rise-time characteristics of the optoacoustic cell, which demonstrated a $1/e$ rise time of 200 s (3.3 min), and a 90% rise time of 420 s (7 min). The cell was exposed to the 10-ppb mixture for over an hour before the dilution system was programmed for a concentration of 20 ppb in order to generate the second step. Because this programming was performed while the measurements were being made, the second step reveals the combined rise time of the optoacoustic cell and the dilution system, with the latter being predominantly responsible for the increased delay due to the larger overall surface area and number of components that were exposed to the mixture. The $1/e$ rise time for the second step is harder to quantify as the rise time is not truly exponential in nature, but can be estimated as being between 450 and 500 s (~ 7.5 – 8.3 min). The 90% rise time was approximately 1700 s (~ 28 min). Note that

the plateau values were never fully achieved in this experiment, and can take hours to reach after the 90% value is surpassed.

The last 25–30 min of each measurement plateau were flat enough for estimating the sensitivity of the instrument. The average value and standard deviation of the measured concentration with a 30-s integration time and 2 W of laser power were 9.58 ± 0.22 ppb for the first plateau and 20.75 ± 0.40 ppb for the second plateau. At both measurement plateaus, the precision was less than 2% of the measured value, and thus, as the measurement value increases, the absolute scatter will correspondingly increase. The accuracy is approximately 4%, which is most likely limited by the ability of the mass flow controllers to accurately generate the desired mixture. The background signal from window absorption produced < 1 ppb of equivalent ammonia signal and was stable over time, and thus was accounted for by subtraction with every measurement. This value for window-noise equivalent signal is much better than that given in prior work [9], which had roughly 300 ppb equivalent window noise, despite the inclusion of acoustic baffles and other elements that were designed specifically to suppress window noise. In contrast, the smaller window signal for this work was achieved using simple acoustic buffers and optimized optical alignment.

By treating the 220-ppt precision for measurements of 10 ppb NH_3 as a conservative estimate of the instrument's minimum detectivity for a 30-s measurement, the minimum detectable optical density, $\alpha_{\min}l$, is calculated to be 2.0×10^{-7} , the minimum detectable absorption coefficient, α_{\min} , is $2.2 \times 10^{-8} \text{ cm}^{-1}$, and the minimum detectable absorption coefficient normalized by power and bandwidth is $2.4 \times 10^{-7} \text{ W cm}^{-1}/\sqrt{\text{Hz}}$. Prior publications using similar resonant strategies report values with better normalized minimum detectable absorption coefficients ($1.4 \times 10^{-9} \text{ W cm}^{-1}$ by Schmohl et al. in the near-infrared [10], and $1.3 \times 10^{-8} \text{ W cm}^{-1}/\sqrt{\text{Hz}}$ by Henningsen et al. using the same CO_2 laser transition as reported for this work [9]), but worse actual detection limits because they used lower power lasers or different measurement conditions. Note that for both of these prior publications, the authors did not demonstrate the minimum detection limits by measuring the standard deviation from successive measurements with concentrations near the detection limit; rather, the detection limits were estimated from signal-to-noise ratios at much higher concentrations (5 ppm and higher for Schmohl et al. and 1 ppm and higher for Henningsen et al.), and then extrapolated down for lower concentrations. Though signal-to-noise ratio estimates at these higher concentrations are useful parameters, an instrument's true sensitivity is determined by the repeatability with which it measures the same concentration.

7 Conclusions

We have developed a sensor for detecting trace concentrations of ammonia in industrial settings using CO_2 lasers and photoacoustic spectroscopy. The CO_2 laser was operated at its $9R(30)$ transition near $9.22 \mu\text{m}$ to interrogate the strong $sR(5, K)$ multiplet of ammonia at the same approximate wavelength with 2 W of output power. The natural resonance of the sample cell's first longitudinal mode, which had a quality factor of 49.7 near 1915 Hz, was used to enhance the signal, yielding an overall cell factor of 3250 Pa cm/W . Background signals from window absorption were < 1 ppb, which represents a substantial improvement over prior work for a similar approach. These sensors can detect ammonia with an estimated sensitivity of 220 ppt in an integration time of 30 s and with excellent linearity over a wide range of concentrations. An optically multiplexed configuration was used to make measurements in four cells, thereby demonstrating the capacity of photoacoustic spectroscopy to make measurements in different sample streams simultaneously using the same laser. These results represent, to the best of our knowledge, the first published demonstration of optical multiplexing for simultaneous photoacoustic measurements of multiple sample streams.

ACKNOWLEDGEMENTS The authors would like to acknowledge the contributions of B. Koraiшы, T.N. MacDonald and B.D. Wiemeyer.

REFERENCES

- 1 J.H. Seinfeld, S.N. Pandis: *Atmospheric Chemistry and Physics: From Air Pollution to Climate Change* (Wiley, New York 1997)
- 2 S. MacDonald, N. Clecak, R. Wendt, C.G. Willson, C. Snyder, C. Knors, N. Deyoe, J. Maltabes, J. Morrow, A. McGuire, S. Holmes: "Airborne Chemical Contamination of a Chemically Amplified Resist". *Proc SPIE* **1466**, 2 (1991)
- 3 D. Kinkad, M. Joffe, J. Higley, O. Kishkovich: Technology Transfer No. 95052812A-TR, SEMATECH (1995)
- 4 P. Hess (Ed.): *Topics in Current Physics: Photoacoustic, Photothermal and Photochemical Processes in Gases* (Springer-Verlag, Berlin 1989)
- 5 P. Repond, M.W. Sigrist: *Appl. Opt.* **35**, 4065 (1996)
- 6 A. Miklos, P. Hess: *Rev. Sci. Instrum.* **72**, 1937 (2001)
- 7 S. Schafer, A. Miklos, P. Hess: *Appl. Opt.* **36**, 3202 (1997)
- 8 W. Demtroder: *Laser Spectroscopy: Basic Concepts and Instrumentation*, 2nd edn. (Springer-Verlag, Berlin 1996)
- 9 J. Henningsen, N. Melander: *Appl. Opt.* **36**, 7037 (1997)
- 10 A. Schmohl, A. Miklos, P. Hess: *Appl. Opt.* **41**, 1815 (2002)
- 11 L.B. Kreuzer, N.D. Kenyon, C.K.N. Patel: *Science* **177**, 347 (1972)
- 12 L.S. Rothmann, C.P. Rinsland, A. Goldman, S.T. Massie, D.P. Edwards, J.Y. Mandin, J. Schroeder, A. McCann, R.R. Gamache, R.B. Wattsin, K. Yoshino, K.V. Chance, K.W. Juck, L.R. Brown, V. Nemtchechin, P. Varanasi: *J. Quant. Spectrosc. Radiat. Transfer* **60**, 710 (1998)
- 13 S.M. Beck: *Appl. Opt.* **24**, 1761 (1985)
- 14 N. Melander, J. Henningsen: 'A photoacoustic study of adsorption'. *AIP Conf. Proc.* **463**, 78 (1999)
- 15 A. Schmohl, A. Miklos, P. Hess: *Appl. Opt.* **40**, 2571 (2001)